https://doi.org/10.1590/s1413-41522023135

Scientific Paper

Removal of H2S from biogas by adsorption with commercial activated carbon and granular iron oxide

Remoção de H2S de biogas por adsorção em carvão ativado comercial e oxido de ferro granular

Isabela Da Cruz Bonatto[1], Hugo Rohden Becker[1], Marcelo Seleme Matias[1]*,
Paulo Belli Filho[1], Armando Borges de Castilhos Júnior[1]

ABSTRACT

Among the impurities that are harmful to the energy conversion of biogas generated in landfills is hydrogen sulfide (H_2S). The present study compared the efficiency of H_2S removal with the use of granular activated carbon (GAC) of two commercial brands, Norit GAC and Pelegrini GAC, and with the use of granular iron oxide from mineral residues. The tests were conducted on a laboratory scale, in a glass column, filled with filtering material, applying an inlet flow of gas and monitoring the outlet concentration. The best removal efficiencies occurred with the use of Norit GAC, which presented longer rupture times. Wet gas tests were also carried out, in which rupture and equilibrium times increased with the use of Norit GAC, while with the use of Pelegrini GAC the same adsorptive behavior was not observed. Tests with iron oxide showed low potential for H_2S removal due to reduced specific surface values, although it provided removal of the contaminant. Knowledge of the saturation time and adsorption equilibrium data is essential for a better understanding and planning of adsorption systems, in addition to the conduction of studies on the influence of external factors and variations in initial concentration.

Keywords: biogas; treatment; landfill; removal of hydrogen sulfide; activated carbon; iron oxide.

RESUMO

Dentre as impurezas prejudiciais à conversão energética do biogás gerado em aterros sanitários, encontra-se o sulfeto de hidrogênio (H_2S). Este trabalho comparou a eficiência de remoção de H_2S com o uso de carvão ativado granular (CAG) de duas marcas comerciais, CAG Norit e CAG Pelegrini, e com o uso de óxido de ferro granular proveniente de resíduos minerais. Os ensaios foram conduzidos em escala laboratorial, em coluna de vidro, preenchida com material filtrante, aplicando-se fluxo de entrada de gás e monitorando-se a concentração de saída. As melhores eficiências de remoção ocorreram com o uso do CAG Norit, que apresentou maiores tempos de ruptura. Também foram realizados ensaios com gás úmido, em que os tempos de ruptura e de equilíbrio aumentaram com o uso do CAG Norit, enquanto com o uso de CAG Pelegrini não se visualizou o mesmo comportamento adsortivo. Os ensaios com óxido de ferro mostraram baixo potencial de remoção de H_2S, devido aos valores reduzidos de superfície específica, embora tenham proporcionado a remoção do contaminante. O conhecimento sobre dados de equilíbrio é fundamental para melhor entendimento e planejamento de sistemas de adsorção, além da inclusão de estudos de influência de fatores externos e de variações de concentração inicial.

Palavras-chave: biogás; remoção de sulfeto de hidrogênio; carvão ativado; óxido de ferro.

INTRODUCTION

Environmental issues are an element of growing concern among the population, even more so in the last decade (CALCULLI *et al.*, 2021). Since the beginning of the 20th century, discussions and studies on issues related to the expenditure of raw material and energy, generating processes and management of solid waste of urban and industrial origin, and the search for new alternatives and technologies go together in an attempt to maintain sustainable development (DIAS, 2002; CALCULLI *et al.*, 2021).

Globally, solid waste growth is projected to be 3.40 billion tons by 2050, more than double the population growth in the same period (KAZA *et al.*, 2018). In this context, concerns about climate change are also growing, particularly as a result of the dispersion of greenhouse gases into the atmosphere.

[1]Universidade Federal de Santa Catarina, Departamento de Engenharia Sanitária e Ambiental – Florianópolis (SC), Brazil.
***Corresponding author:** msmatias.esa@gmail.com

Received on:10/22/2023 – **Accepted on:** 02/27/2024

In many countries, urban solid waste is continuously accumulated in landfills, where these materials are the object of complex biophysicochemical phenomena, resulting in the global production of leachates and biogas (DOS SANTOS *et al.*, 2020). Biogas is a gas mixture composed mainly of methane (CH_4), a greenhouse gas responsible for 25% of global warming, and its concentrations in the atmosphere have more than doubled in the last two centuries, largely due to anthropogenic activities, 11% of these due to urban solid waste (MIRZABAEV *et al.*, 2019). At the same time, the use of these gases consists of a renewable and sustainable energy source (EPA, 2010). In addition to the main constituent, biogas also has carbon dioxide (CO_2) and small amounts of water vapor, as well as other elements considered as impurities, such as hydrogen sulfide (H_2S) and siloxanes. Due to its corrosive nature, hydrogen sulfide is one of the elements that must be removed from biogas before the energy conversion process (CURIEL-ESPARZA *et al.*, 2019). Thus, several biogas purification techniques have been developed in order to enhance the use of biogas (CRISTIANO *et al.*, 2020).

Purification can be carried out through biological, chemical, and/or physical processes. Adsorption using activated carbon and iron oxide is one of these methods, which has the ability to selectively adsorb compounds and remove them from the mixture. In Brazil, considering the use of biogas as biomethane, specifications for biogas quality, which includes H_2S, are provided for in the Resolution by the National Agency for Petroleum, Natural Gas, and Biofuels — ANP (ANP, 2015).

The present study compared different processes of biogas purification/removal of H_2S by adsorption using different commercial species of activated carbon and granular iron oxide originating from tailings from coal mining.

LITERATURE REVIEW

One of the methods commonly used and considered economically viable for the reality of many countries is landfill disposal (HU, DU and LONG, 2017; LIMA *et al.*, 2018). Inside a sanitary landfill, waste degradation occurs basically in three ways: through the dissolution of mineral elements present in the environment; due to the carrying of fine particles and soluble material by the percolation water; and mainly due to the bioconversion of organic matter into soluble and gaseous forms, under the influence of physical, chemical, and biological mechanisms resulting from the interaction between components from the waste itself and between natural agents (water and microorganisms) (CASTILHOS JUNIOR *et al.*, 2003; ZANTA *et al.*, 2006). Solid urban waste continuously accumulated in landfills under the influence of natural agents (rain and microorganisms) degrades by aerobic and/or anaerobic biodegradation processes, resulting in leachates and biogas (GARCILASSO, VELÁZQUEZ and COELHO, 2009; LANGE e AMARAL, 2009).

Biogas is the main product resulting from the anaerobic digestion of landfilled organic matter and its characteristics vary according to the composition of the landfilled waste and its decomposition stage, which can be subdivided into four subsequent phases: hydrolysis, acidogenesis, acetogenesis, and methanogenesis (METCALF and EDDY, 1991; CHERNICHARO, 1997; PELCZAR JUNIOR, CHAN and KRIEG, 1997; ALVES, 2007).

Typically, biogas is composed of 60% methane, 35% carbon dioxide, and 5% of a mixture of other gases such as hydrogen, nitrogen, hydrogen sulfide, carbon monoxide, ammonia, oxygen, and volatile amines (PECORA, 2006). Occasionally, traces of organic compounds of sulfur, halogenated hydrocarbons, hydrogen, nitrogen, carbon monoxide, and oxygen are observed, which can be toxic (PELLERIN *et al.*, 1988; REICHERT, 2007). A gaseous mixture saturated with water vapor may contain dust particles and siloxanes (WELLINGER and LINBERG, 2000). Its concentration in biogas depends on the raw material and can vary between 0.1 to 2% (BOYD, 2000; LASTELLA *et al.*, 2002). These gases present in smaller quantities influence the choice of operation, cleaning, and combustion technology (PECORA, 2006).

Pizarro-Loiaza *et al.* (2021) and Mercado (2010) cite some energy benefits of biogas conversion: it is a renewable energy source, a high quality fuel, and the combustion of methane produces water and carbon dioxide, generating no toxic gas—which can bring environmental, economic, social, and human health benefits. In addition, when choosing cogeneration systems, i.e. combined heat and power production, part of the electricity can be used in the facilities themselves and part can be commercialized.

Biogas produced by biomass residues has become one of the most important alternative energy sources in recent years, as it is derived from non-fossil sources (KANG *et al.*, 2010; PIZARRO-LOAIZA *et al.*, 2021), reducing nutrient and greenhouse gas emissions (AYODELE, OGUNJUYIGBE and ALAO, 2018; PIZARRO-LOAIZA *et al.*, 2021). There are several technologies to perform the energy conversion of biogas. However, gas purification systems must be provided in order to correct the natural properties of biogas and reduce the content of unwanted gases, so that it meets the technical specifications of efficiency equipment (OLIVEIRA and CARVALHO, 2005).

According to Alves (2000), the presence of non-combustible substances in biogas, such as water and/or carbon dioxide, impairs the burning process, making it less efficient. In addition, the use of biogas can also be limited by the amount of hydrogen sulfide that it contains, given that, due to its corrosive nature, it becomes harmful to the internal parts of combustion engines (TCHOBANOGLOUS, BURTON and STENSEL, 2003) and reduces the service life of pipelines and other installations required for biogas utilization (DÍAZ *et al.*, 2010). The biogas technologies market is in a development stage, with derivations of gas treatment and separation methodologies, mainly from natural gas treatment. Biogas can be upgraded to natural gas standards by gas absorption, adsorption, and permeation processes. Current biogas treatment technologies may include, for example, pressure oscillation adsorption, chemical washing, water washing, organic solvent washing, membrane separation, and cryogenic separation. The selection of the appropriate technology to update the raw biogas depends on its end use, the economy involved, and the efficiency of the purification process (KHAN *et al.*, 2021). Currently, the main treatment processes focus on chemical absorption, physical absorption, physical and chemical absorption, and direct oxidation (CAO *et al.*, 2021).

In the use of adsorption methods, there are substances that act as adsorbents, fixing other substances on their surface. Adsorbents depend on the physical adsorption of a molecule in the gas phase on a solid surface. High porosity and large surface areas are desirable characteristics for adsorbent solids, allowing larger physical areas for adsorption to occur. The medium eventually becomes saturated and needs to be replaced or regenerated (YANG, 1987). Activated carbon is an adsorbent material known for its high removal efficiency, low reuse costs and possible product recovery (HERNÁNDEZ *et al.*, 2011).

In the treatment of effluent, the application of activated carbon can be carried out in two ways: using powder activated carbon (PAC) or in the form of granular activated carbon (GAC). Although there may be some limitations regarding PAC application when compared to GAC, its main advantage is that, depending on the variability of the raw effluent characteristics, it is possible to correct the PAC dosage in such a way as to maximize the removal efficiency of any adsorbate, or just apply it sporadically, when necessary (HOWARD, 1989). In general, activated carbon has a high adsorption capacity for this purpose, but its high cost and the impossibility of reuse has led to a search for alternative materials that are more easily accessible, so the materials frequently used are nanoporous (PELUSO *et al.*, 2019).

Other alternatives to the use of activated carbon are natural materials (wood, peat, charcoal, lignite), industrial, agricultural or residential waste or by-products, or products such as blast furnace slag, bagasse fly ash or red mud (THANAKUNPAISIT, JANTARACHAT and ONTHONG, 2017). Another adsorbent material is iron oxide, which can also perform the removal of hydrogen sulfide by adsorption, with the formation of iron sulfide, so that the material can still be regenerated with the use of oxygen, thus obtaining elemental sulfur and, again, iron oxide (MUCHE and ZIMMERMANN, 1984). Among the materials used, commonly there is iron oxide and iron hydroxide, which capture hydrogen sulfide on their surface, forming iron sulfide and water (ABATZOGLOU and BOIVIN, 2008). Iron oxide nanoparticles alone or together with other metal oxides are also alternatives for reducing H_2S concentrations, even during the anaerobic digestion phase of biogas (FARGHALI *et al.*, 2019; ZHANG *et al.*, 2020).

Deublein and Steinhauser (2011) explain that, for a gas treatment apparatus, elements containing oxide and/or iron hydroxide are stacked in layers in a column, which can be either iron wool, iron impregnated wood chips, or iron impregnated pellets. Biogas flows in a perpendicular direction to the layers inside the column, promoting the removal of H_2S by adsorption. Commercial versions of the product manufactured by chemical synthesis can also be found, in pellet format, with great adsorption capacity and good moisture resistance. There are also commercial products in tablet format with a large surface area that promotes a large H_2S removal capacity.

MATERIALS AND METHODS

The study was based on the steps shown in Figure 1. Initially, characterization of the adsorbent materials used was carried out, both by scanning electron microscopy (SEM) and by surface and porosity analysis (BET). Then, the bench tests were carried out using an experimental apparatus where preliminary tests were conducted to define the key parameters used in the definitive tests.

Adsorbent materials used

As for the activated coals used, two commercial brands of GAC — Norit and Pelegrini — were selected, given the manufacturers' representativeness in the commercial and bibliographic scenario, in addition to them being easy to obtain. These carbons are adapted to combine high adsorption capacity, minimal screening effects for large impurities, good adsorption kinetics, low retentivity, and good thermal conductivity (Figures 2A and 2B). The main characteristics of the materials used in the study are shown in Table 1.

The adsorption tests with iron oxide were carried out with adsorbent material from the process of obtaining sulfuric acid (H_2SO_4) from the ustulation of carbonaceous pyrite. The iron oxide used is a by-product of this process, since carbonaceous pyrite contains 98% of hematite (FeO_3). Given that it was initially in powdery form, it was necessary for the material to undergo a grain formation process, so that it could be used in the experiment (Figure 2C). Through sieving, specific granulometries (2.00 to 4.70 mm) were adopted for different tests.

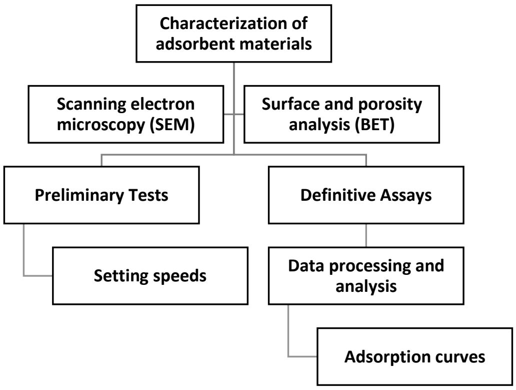

Source: elaborated by the authors (2023).

Figure 1 – Methodological steps adopted in the study.

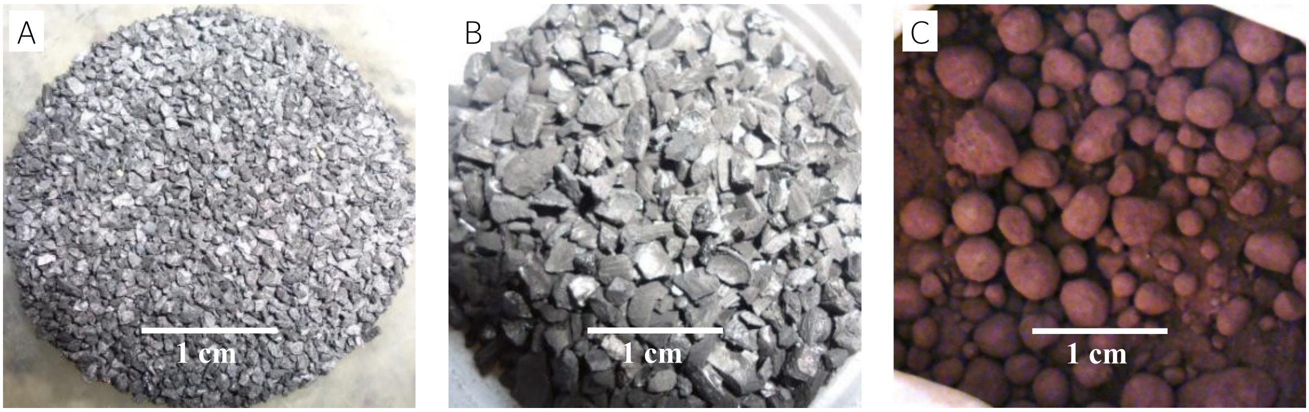

Source: elaborated by the authors (2023).

Figure 2 – Materials used in the study: (A) Norit GAC; (B) Pelegrini GAC; (C) Iron oxide.

Characterization of the materials

Surface area analysis

The BET surface area of all adsorbent materials used was evaluated. The assessment was carried out with and without prior treatment, which consisted of washing the samples with deionized water and drying them for 12 hours at a temperature of 250°C. Thus, for the GAC, four samples were separated, named Norit 1 (without pretreatment); Norit 2 (with pretreatment); Pelegrini 1 (without pretreatment); and Pelegrini 2 (with pretreatment). This separation occurred only for the analysis of surface area and porosity, to verify if there would be differences in the results of the materials' characteristics. For the adsorption experiments, the materials were used without pretreatment, directly from commercial packaging. For iron oxide, the samples were separated into granular iron oxide and powdered iron oxide. Surface area analyses were performed for the adsorbent material in granular format. For the powdery form, only the surface area was determined. For the analysis, the desired values of relative pressure were established during the test, and the sample was kept at the boiling temperature of liquid nitrogen (-196°C). The samples were subjected to a small flow of gaseous N_2 and, with the gradual increase in its pressure, the gas was adsorbed by the sample. The volume of adsorbed N_2 was measured after each equilibrium was achieved. After adsorption, desorption was carried out, which made it possible to build an adsorption-desorption curve for N_2, allowing the calculation of the surface area, volume, and width of the micropores. After the end of the analysis, the samples were weighed again. All the data obtained were analyzed using the equipment Quantachrome, model Nova 2200e, in the computer program Quantachrome NovaWin-Data Acquisition and Reduction for NOVA instruments, version 10.1.

Scanning electron microscopy and energy dispersive x-ray spectroscopy

Through SEM analysis it was possible to analyze the morphological structures and basic chemical elements in the two commercial brands of GAC and the iron oxide. The morphology analysis of the materials was performed by means of a scanning electron microscope, model JSM-5510, Jeol brand, coupled with an energy dispersive x-ray spectroscopy (EDX) system. A line element analysis was also carried out, as a result of the EDX system, with the elemental composition and concentration being demonstrated. In order to investigate a possible morphological or chemical element difference, we chose to use, for each material, a virgin sample and a saturated sample after use in the adsorption tests. The samples were prepared by their metallization. A minimum aliquot was added to a double-sided carbon tape, responsible for conducting and flowing electrons from the microscope beam. Then, through the use of an evaporator, model JEE4C, a nanometric layer of gold was deposited on the sample. The already metallized samples were taken to the electron microscope to scan the images. The data were processed in the "System six" software, also from the manufacturer ThermoNoran.

Table 1 – Main characteristics of the materials used.

	NORIT	PELEGRINI
Raw material	Bitumen (mineral)	Coconut shell (vegetable)
Activation	Physics with steam	Physics with water vapor and heat (960°C)
Granulometry	0.6 to 1.7 mm	2 to 3.5 mm
Minimum iodine	900 mg/g	700 mg/g
Humidity (maximum)	5%	8%
Apparent density	470 kg/m³	500 kg/m³
Hardness (minimum)	97%	95%
Total surface area	1100 m²/g	Not informed

Procedures and experimental apparatus

Tests to remove H_2S from the gas were carried out by submitting a flow of synthetic gas mixture through a glass column filled with adsorbent material, at the average ambient temperature of 25°C and ambient pressure of 1 atm. The concentrations of hydrogen sulfide at the column exit were measured. Once the column output concentration was equal to the input concentration, the saturation of activated carbon by hydrogen sulfide was completed. Through the experimental apparatus, preliminary tests were carried out to identify parameter influences (adsorption column height, gas velocity, humidity, etc.), as shown below. The adsorption tests were carried out by a system built on a laboratory scale in an experimental apparatus based on Cristiano *et al*. (2020) (Figure 3) consisting of a glass column with an internal diameter of 1.5 cm and a height of 60 cm, where a height of 40 cm is available for use. Variations in these dimensions were tested in preliminary trials. The column was coupled to a cylinder with a mixture of synthetic gas for testing (containing H_2S in concentration of 200 ppmv and balance in N_2). The gas flow was controlled by fine adjustment valves and an Omel brand rotameter, with a measuring range from 0 to 500 $Nl.h^{-1}$. Gases entered from the bottom of the column, passing through a perforated support to sustain the substrate and ensure its uniform distribution. The measurement of H_2S concentration at the output of the column was performed with the use of Landtec GEM 2000 equipment, which had a coupled cell for measuring H_2S, with a measuring range of 0 – 200 ppmv.

In order to determine the experimental conditions, preliminary tests were carried out, evaluating the efficiency of H_2S removal over time by different velocities found in the literature. Once the analyses were performed, the percentage of H_2S removal was identified, according to the difference between the initial and final concentrations, after passing through the column. For each test, material

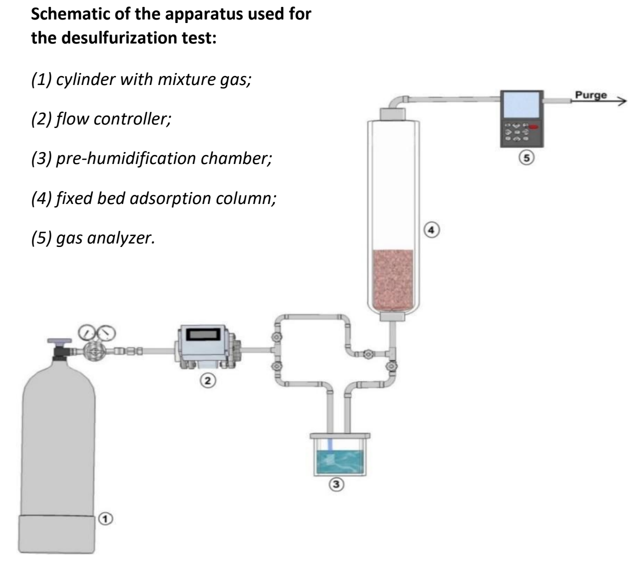
Schematic of the apparatus used for the desulfurization test:

(1) cylinder with mixture gas;

(2) flow controller;

(3) pre-humidification chamber;

(4) fixed bed adsorption column;

(5) gas analyzer.

Source: modified from Cristiano *et al.* (2020).

Figure 3 – Experimental apparatus used in the study.

saturation curves were generated, with the output concentration of H_2S (in ppm) over time (in minutes). Triplicate assays were carried out for each assay. For the GAC, the established height of the column was 5 cm, at speeds of 3.5, 6.5, and 10.0 $cm.s^{-1}$. Tests were also carried out with humidified gas in relation to the two linear velocities that best presented efficiency of H_2S retention, making the gas flow through a flask with water. Water saturation was awaited before sending the humidified gas to the inlet at the bottom of the column. Preliminary tests were carried out for iron oxide at velocities of 1.0, 2.5, and 5.0 $cm.s^{-1}$, for three different heights of material in the column: 7.5, 15.0, and 30.0 cm. For the definitive tests with iron oxide, a finer granulometry was sought, depending on the conclusions obtained from the preliminary tests (2.00 to 4.70 mm).

Curves and adsorption capacity

Through the monitored data it was possible to construct adsorption curves to evaluate the adsorption capacity of the adsorbents. The curves were created considering the relationship between the output concentration and the initial concentration (200 ppmv H_2S) over time. The rupture curves consist of obtaining the adsorption behavior on the adsorbent in a fixed bed column over time, considering the effects of dispersion and mass transfer, up to its total saturation (equilibrium). Dueto the large adsorption capacity of the adsorbent, the rupture curves were obtained until the adsorbate concentration (H_2S) at the output of the column (C_s) reached approximately 90% of the input concentration (C_o), i.e. $C/C_o = 0{,}9$. To obtain the total saturation time, that is, when $C_s/C_o = 1$, a long adsorption follow-up time would be necessary, with excessive use of synthetic gas. Analysis of the adsorption curve also showed the rupture time (tr), which corresponds to the time from which the bed begins to saturate and the solute is detected at the output of the fixed bed ($C_S \approx 10\%\ C_o$). The best process efficiency corresponded to the longest rupture time. The amount of adsorbate per unit mass of adsorbent material obtained over time was calculated according to Equation 1, where the accumulated sum of these values, recorded every 2 minutes, resulted in the retention of H_2S at the end of the experiment. This capacity was calculated for the average of all conditions.

$$q = \frac{C_o - C_s}{m} . v \tag{1}$$

Where: C_o: initial concentration of adsorbate (g/m^3); C_s: output concentration measured by GEM 2000 ($g.\ m^{-3}$); v: volume of gas in contact with the adsorbent ($m^3.\ min^{-1}$); and m: mass of the adsorbent material (g).

RESULTS AND DISCUSSIONS

Characterization of the materials

Surface area analysis

For the CAG, the highest surface area values were found for the Norit samples, as can be seen in Table 2. For both brands, the highest values were found when there was pretreatment, evidencing its importance before the use of these materials, which can significantly improve adsorption.

As for iron oxide, the results of the surface area analysis by the BET method showed that the sample of granular iron oxide with previous treatment was the one that presented the highest surface area value — 11.49 $m^2.g^{-1}$ (Table 2). However, the result found for the surface area of granular iron oxide demonstrates that the value of 11.49 $m^2.g^{-1}$ is low and indicates that the material does not have a large H_2S removal capacity. The results demonstrate that pretreatment is essential for the removal of impurities from the pores and surface of the adsorbent, making the material have a greater surface area available for use.

Morphology with scanning electron microscopy

Visualization of the GAC samples by means of SEM showed little difference in the surface morphology of the samples. Norit CAG samples presented more homogeneous pores (Figure 4) than those of Pelegrini GAC, which appeared to have more heterogeneous pores, of different sizes and certain surface irregularity, as can be seen in Figure 5. In relation to differences between saturated and unsaturated samples, none were observed for any of the brands. This implies that saturation by H_2S in these granules does not lead to apparent differences in the surface morphology of these adsorbent materials.

The powdered iron oxide, virgin, and saturated samples show differences that can be seen in Figures 6A and 6B. Figure 6A shows homogeneous pores in large parts of the sample. The saturation of granular iron oxide can be observed in Figure 6B, where a darkening of the image is seen throughout the sample. Figure 7B confirms an accumulation due to sulfur adsorption in the granular

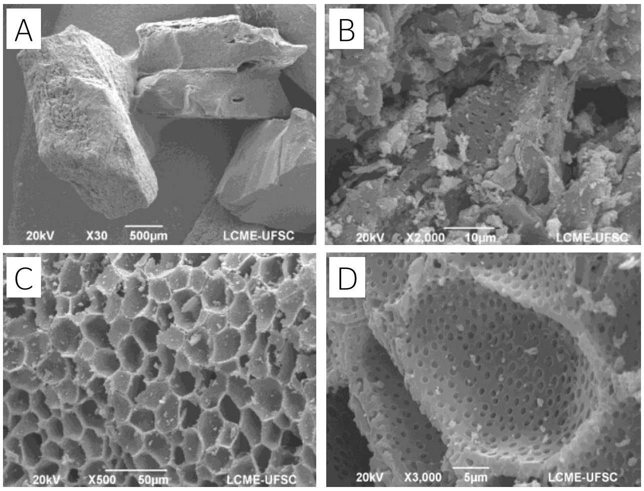

Source: elaborated by the authors (2023).

Figure 4 – NORIT virgin activated carbon granules with magnification of 30x (A) and 2,000x (B) and NORIT saturated activated carbon granules with magnification of 500x (C) and 3,000x (D).

Table 2 – Surface area values (m^2/g) found in the tests carried out for the different samples.

Material/parameters	Norit GAC		Pelegrini GAC		Iron oxide	
Pretreatment	No prior treatment	With prior treatment	No prior treatment	With prior treatment	No prior treatment	With prior treatment
Multi-Point BET ($m^2.g^{-1}$)	782.83	822.98	49.77	485.73	6.08	11.49

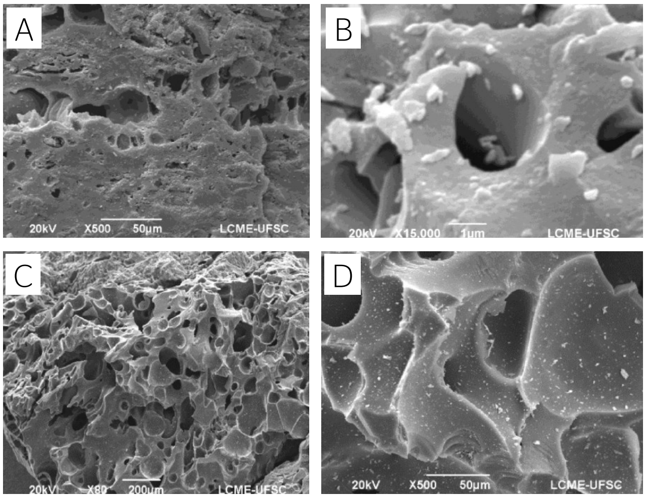

Source: elaborated by the authors (2023).

Figure 5 – Virgin Pelegrini activated carbon granules with 500x magnification (A), 15,000x (B) and saturated Pelegrini activated carbon granules with 80x magnification (C) and 500x (D).

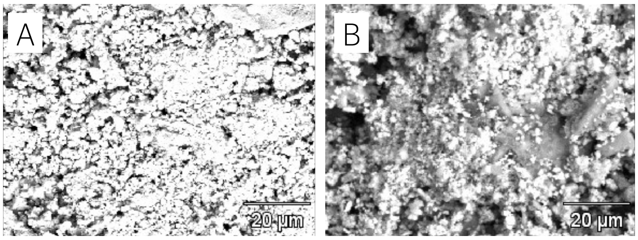

Source: elaborated by the authors (2023).

Figure 6 – Scanning electron microscopy images of (A) virgin granular iron oxide with 1,000x magnification, (B) saturated granular iron oxide with 1,000x magnification.

iron oxide sample, since this SEM image was produced to obtain only the presence of the sulfur element. In Figure 7B, three regions in the sample (highlighted) with higher concentration of points are evidenced. In Figure 7A, this concentration of points does not occur.

As for the Line Element analysis, from the energy bands the differences between the chemical elements in the samples (carbon, sulfur, and oxygen) were demonstrated. The results of this analysis are shown in Table 3.

The amount of carbon was similar for the two virgin activated carbon brands, and these quantities declined both in weight and in the presence of the atom after the saturation process. Oxygen quantities increased after saturation for both brands, while sulfur was only observed after saturation for Pelegrini material, remaining at zero in all other cases. In relation to iron oxide, the results of the analysis showed that there was an increase of 58.9% in the presence of sulfur in the saturated material, which shows an accumulation of sulfur on the surface of the saturated sample as a result of the adsorption of H_2S in iron oxide (Table 3).

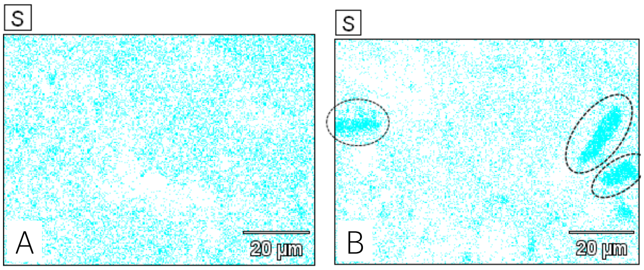

Source: elaborated by the authors (2023).

Figure 7 – Scanning electron microscopy images for analysis of the sulfur element of (A) virgin granular iron oxide with 1,000x magnification, (B) saturated granular iron oxide with 1,000x magnification.

Table 3 – Results of the line element analysis for each sample.

Sample		Element	Element weight (%)	Error ±	Presence of the atom (%)	Error ±
NORIT GAC	Virgin	Carbon	73.34	2.28	85.77	2.65
		Oxygen	4.99	0.75	4.38	0.67
		Sulfur	0	0	0	0
	Saturated	Carbon	53.59	0.87	58.09	0.95
		Oxygen	10.32	1.62	8.40	1.32
		Sulfur	0	0	0	0
Pelegrini GAC	Virgin	Carbon	73.13	0.55	80.4	0.61
		Oxygen	7.33	0.57	6.05	0.47
		Sulfur	0	0	0	0
	Saturated	Carbon	59.13	0.63	68.21	0.73
		Oxygen	11.14	0.38	9.65	0.33
		Sulfur	5.16	0.17	2.23	0.07
Iron oxide	Virgin	Carbon	8.55	0.38	25.29	1.13
		Oxygen	8.96	0.15	18.89	0.33
		Sulfur	1.29	0.14	1.43	0.15
	Saturated	Carbon	3.81	0.23	11.01	0.67
		Oxygen	15.04	0.12	32.62	0.27
		Sulfur	2.05	0.05	2.22	0.06

Test results and adsorption capacity

Graphs of the adsorption curves obtained during the adsorption tests are presented below, according to the linear velocities and heights presented in Table4. Triplicates were carried out for each assay. The triplicates of the tests are graphically presented below, in the form of their averages. The results of each triplicate are available in the supplementary materials.

As for the GAC, Norit presents the same typical forms of the adsorption curves, as can be seen in the graph with the average curves for this material (Figure 8), with the only differences in the curves being the time to reach 100% saturation of the material and the rupture times, which are different for each linear speed. The same figure shows a certain similarity with a type V isotherm curve (MURANAKA, 2010), which occurs in microporous adsorbents with a formation of multilayers from low concentrations.

For Pelegrini GAC, the averages curves follow a slightly different behavior trend, with shorter removal times with 100% efficiency and not presenting a sharp start for the rupture time, as can be seen in Figure 9. The time to the complete saturation of Pelegrini GAC is greater, but Norit GAC has longer durations in minutes with 100% removal efficiency, that is, longer times to reach the rupture point, which can be more interesting for biogas purification processes. The shape of the rupture curves is related to internal diffusion and eventually external transfer, axial arrangement, and adsorption isotherm (MURANAKA, 2010).

The difference between the materials may be related to the pore size distribution of the samples. Results obtained by Lozano *et al.* (2002) revealed that a sample with a high volume of micropores and BET surface area, but with dispersed pore size distribution, has a lower adsorption capacity than a sample with smaller BET areas and a smaller volume of micropores. As for iron oxide (Figure 10), there is a direct relationship between gas holding time and the duration of the assay.

Truong and Abatzoglou (2005) observed in their assays that it was not possible to guarantee the reproducibility of the tests, since the granular iron oxide used in the experiments was of a fragile nature, therefore it was difficult to ensure that each filling of the column would result in an identical configuration in the arrangement of the iron oxide grains. This explanation applies to experiments where different saturation curves were observed in the triplicates. The granular iron oxide used, due to the process of grain formation, is brittle. The aim was to maintain grain uniformity in each column filling, but, in some cases, the resulting saturation curves differed from the others, as occurred for a linear velocity of 5.0 cm.s^{-1} and height of 30 cm, and a linear velocity of 2.5 cm.s^{-1} and height of 30 cm.

In a pressure swing adsorption (PSA) process, gas molecules are considered to be adsorbed on an adsorbent material based on their molecular sizes (SUN *et al.*, 2015). Thus, due to its larger size, CH_4 can be separated from CO_2 and it does not adsorb on the adsorbent due to its larger molecular size, being collected at the top of the adsorption column at low pressure (KHAN *et al.*, 2021).

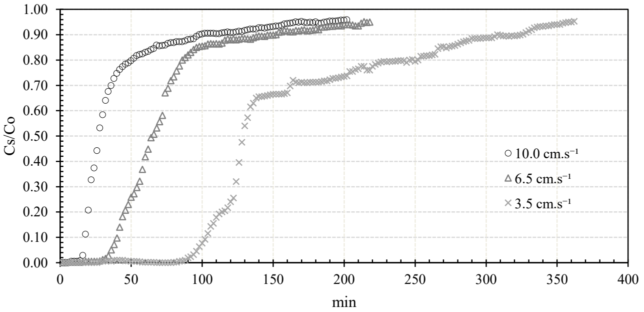

Source: elaborated by the authors (2023).
C_s: gas output concentration; C_o: gas input concentration.

Figure 8 – Average adsorption curves for Norit granular activated carbon with gas without pre-humidification, at speeds 10, 6.5, and 3.5 cm.s^{-1}.

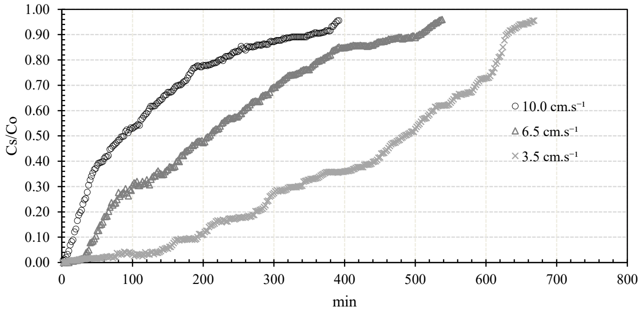

Source: elaborated by the authors (2023).
C_s: gas output concentration; C_o: gas input concentration.

Figure 9 – Average adsorption curves for Pelegrini granular activated carbon with gas without pre-humidification, at velocities of 10, 6.5, and 3.5 cm.s^{-1}.

Table 4 – Average time to achieve removal efficiency of 90% and adsorption capacity per adsorbent mass.

Adsorbent material	Linear Speed (cm.s^{-1})	Column height (cm)	Time to 90% removal (min)	Adsorption capacity (mgH_2S. g^{-1})
Norit GAC	3.5	5.0	308	42.99
	6.5	5.0	152	36.67
	10.0	5.0	98	32.38
Pelegrini GAC	3.5	5.0	630	113.95
	6.5	5.0	506	108.74
	10.0	5.0	354	93.40
Iron oxide	5.0	15.0	140	0.16
	5.0	30.0	226	0.23
	2.5	15.0	246	0.18
	2.5	30.0	347	0.20
	1.0	7.5	692	0.21

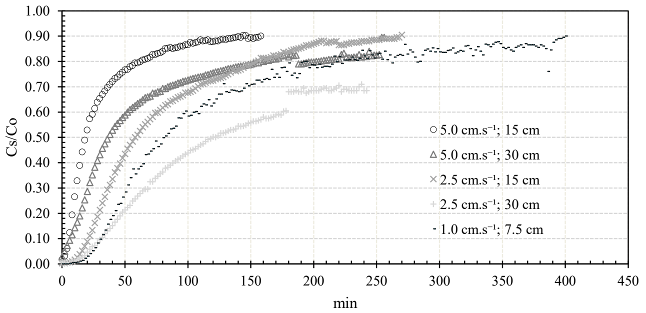

Source: elaborated by the authors (2023).
C_s: gas output concentration; C_o: gas input concentration.

Figure 10 – Average adsorption curves for iron oxide with gas without pre-humidification, at velocities of 5, 2.5, and 1 cm.s^{-1}.

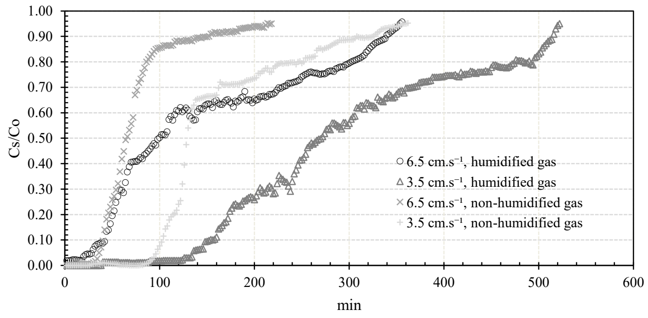

Source: elaborated by the authors (2023).
C_s: gas output concentration; C_o: gas input concentration.

Figure 11 – Average adsorption curves for Norit granular activated carbon, with and without humidification.

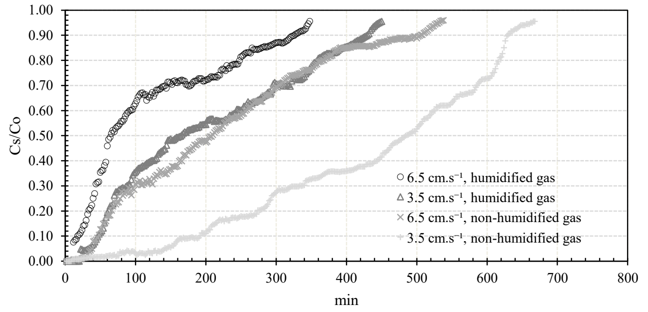

Source: elaborated by the authors (2023).
C_s: gas output concentration; C_o: gas input concentration.

Figure 12 – Average adsorption curves for Pelegrini granular activated carbon, with and without humidification.

Advances in materials technology can also offer adsorbents higher adsorption capacity, greater selectivity, and possibly higher heat resistance. This will allow for better separation efficiency and a higher degree of process integration (KHAN *et al.*, 2021). Since iron oxide has not undergone improvements in its adsorption capacity to actually be marketed as an adsorbent material, this may justify its lower performance when compared to activated coals, which really are commercial products for this purpose and can be used even with water and wet systems; this was not feasible for the iron oxide used in the experiments.

Currently, extensive research work has been devoted to designing and synthesizing adsorbents with the aim of improving their use for the treatment and purification of biogas (FAKHRAIE *et al.*, 2021),

Therefore, humidification tests were carried out only for the commercial activated coals. Assays with gas pre-humidification for granular iron oxide were discarded as they resulted in an aqueous mixture that clogged the gas passage.

Tests with gas humidification

After checking the best rupture times for both GAC materials, the velocities of 3.5 and 6.5 cm.s^{-1} were chosen, and were repeated for triplicates with the hydrogen sulfide synthetic gas going through a pre-humidification process. The average curves of each triplicate can be seen in Figures 11 and 12. Greater instability and less similarity occurred between repetitions, which can be explained due to the flow control (which, with the passage through water, became more unstable, with greater oscillations being visualized in the rotameter). It is possible that the previous passage through water changed the system's pressures and increased the oscillations of the arrival of gas in the column. The tests showed the same behavior patterns, with longer rupture times for Norit GAC, which occurred less abruptly, indicating that slow adsorption kinetics may occur due to the diffusion of the humidified gas in the pores of the adsorbent.

For Pelegrini GAC there was no increase in the rupture times for the two speeds, also presenting instability. In general, the pre-humidification tests showed longer times to reach equilibrium. For Norit GAC, there was an increase in rupture time. The effect of water vapor is remarkable in adsorption in relation to dry gas. Two possible phenomena can be considered: micropores partially filled with water and inaccessible micropores. Inaccessibility of the micropores may occur because some pathways are blocked by the water that is present in other types of pores (meso and macropores), and may be responsible for the low amounts of gas adsorbed by Pelegrini in these experiments (OLIVEIRA, 2004). In addition, capillarity effects reduce the pore sizes, increasing the pressure formation and vice versa (PERRIN *et al.*, 2003). From the experiments carried out, it was observed that adsorption is faster in the initial stages of the process, while it is slower near equilibrium. This behavior occurs because, at the start, there are a lot of empty sites for adsorption. Over time, the number of empty sites decreases. Also, repulsive forces of the already adsorbed molecules begin to exist, which hinders the adsorption process at the remaining sites (SCHNEIDER, 2008). The determination of pore size and volume is important since it indicates the amount of pores available for the adsorption of molecules with known size (PELEKANI, 2000), which may also be responsible for more or less stable adsorption curves. The presence of micropores substantially influences the adsorption properties because the amount adsorbed on the surface of macropores is negligible compared to that of the micropores (AVOM *et al.*, 1997). Another important factor is chemical characterization, where the presence of groups containing oxygen and hydrogen on the carbon surface strongly affects the adsorption properties (DÍAZ *et al.*, 2005). The origin of these surface groups may be the original raw material, the activation process or the introduction of surface groups after preparation by further treatment (DABROWSKI *et al.*, 2005). The adsorbent surface area is one of the most important factors in these processes, since adsorption is a surface phenomenon. In general, the extent of adsorption is greater when the specific surface area is larger (greater total area available for adsorption). The specific surface area is larger for smaller particles; therefore, the smaller and more porous the material, the greater the availability of sites for adsorption of adsorbate molecules, which may represent the best rupture times for Norit GAC. For larger particles the diffusion resistance is higher and much of the inner surface of the particle is not available for adsorption (SEKAR, SAKTHI and RENGARAJ, 2004). Access to the adsorption sites is facilitated when the particle is smaller, which results in higher adsorption levels (BHATNAGAR and JAIN, 2005). It can be noted that Pelegrini GAC presented the highest amount retained in tests without gas pre-humidification for all linear velocities (2.17 $mol.L^{-1}$ for 3.5 $cm.s^{-1}$; 1.12 $mol.L^{-1}$ for 6.5 $cm.s^{-1}$) than tests with gas pre-humidification (1.01 $mol.L^{-1}$ for 3.5 $cm.s^{-1}$; 0.60 $mol.L^{-1}$ for 6.5 $cm.s^{-1}$). Norit GAC showed better retained amounts in gas humidification tests. Even though, as seen in the adsorption curves, Norit had the best rupture times (28 min for 3.5 $cm.s^{-1}$), the experiments were longer for Pelegrini, which may have influenced this result, which took into account the total time of the experiment. Preliminary tests were performed for granular iron oxide using a pre-humidification process of the adsorbent. In these tests, it was verified that the material would not be able to be humidified, as the contact with moisture resulted in an aqueous mixture with iron oxide, which ended up clogging the gas inlet in the column. Therefore, gas humidification tests for granular iron oxide were discarded. This result is due to the artisanal manufacturing characteristic of the iron oxide grains for this test.

CONCLUSIONS AND RECOMMENDATIONS

The adsorption process in the removal of H_2S using two commercial brands of activated carbon, Norit and Pelegrini, and granular iron oxide was studied. As for the GAC, the imported commercial brand Norit presented better rupture times for H_2S (28 min for 3.5 $cm.s^{-1}$) than the Brazilian national brand Pelegrini (10 min for 3.5 $cm.s^{-1}$). Specific surface analyses also showed superiority in total pore volume and specific area, characteristics that are directly related to the adsorption capacity of adsorbent materials. As noted in the experiments, very low velocities are not enough to overcome the loss of load inside the column, allowing oxygen to enter, which influences the adsorption process. Very high speeds are not interesting either, since, as much as they increase the adsorbed amount instantly, with an increase in pressure in the adsorbent sites, they favor a faster saturation, with shorter rupture times. For the tests carried out, the best linear velocity found was 3.5 $cm.s^{-1}$. In relation to the tests using gas with and without pre-humidification, there was some instability in the flow, which resulted in greater instabilities also in the gas output reading. Norit GAC showed better rupture times when the gas was humidified, behaving in the same way as some authors have also verified. As for Pelegrini, the behavior did not follow the same trend, with better times removing H_2S from 90 to 100% in tests without gas pre-humidification. With regard to iron oxide, the tested material provided the removal of H_2S, which can be proven by the increase of 58.9% in the amount of sulfur detected in both virgin and saturated samples analyzed in SEM. However, the material has reduced values of specific surface, and the result found, of 11.49 $m^2.g^{-1}$, is low, which indicates that it does not have great potential for H_2S removal. The test results showed that the material removal capacity is directly linked to the linear velocity of the gas passing through the column. Assays with gas pre-humidification for granular iron oxide were discarded as they resulted in an aqueous mixture that clogged the gas passage. According to the objective of the experiment, it is necessary to consider that each experimental configuration (column dimensions, gas flow, gas concentration and origin, quantity and characteristics of material used, etc.) requires a specific study and planning, as there can be different dynamics in each system.

Furthermore, the method of designing the adsorbent materials can also reflect on different results for the purification of biogas, so that materials with higher technology for adsorption have better performance in relation to artisanal materials or ones with less treatment.

In the case of the granular iron oxide used in the experiments, its grain formation process occurred by mixing the powdery material with water in a concrete mixer. The artisanal process only ensured the formation of grains necessary for the test in columns, and no other additional treatment was performed.

Several different experimental conditions can be studied, alternating and investigating different parameters such as: adsorbent material, granulometries, adsorption for different pretreatment, other characterization analyses, column configurations, quantities of adsorbent material, tests with more than one initial gas concentration, other synthetic gas mixtures, moisture contents, experimental controls, etc. These are some parameters that can directly alter adsorption processes.

In addition to these parameters, the experiments carried out demonstrated a great difference in the adsorption capacities of commercial activated carbons in comparison with the granular iron oxide, which is a residue. The joint analysis of the H_2S adsorption results, surface area, and pore volume suggests that the iron oxide adopted in this experiment is amenable to complementary studies in order to improve its characteristics, with the aim of achieving adsorption capacity results compatible with those observed with activated carbon.

REFERENCES

ABATZOGLOU, N.; BOIVIN, S. A review of biogas purification processes. *Biofuels, Bioproducts and Biorefining*, v. 3, n. 1, 42-71, 2009. https://doi.org/10.1002/bbb.117

AGÊNCIA NACIONAL DO PETRÓLEO, GÁS NATURAL E BIOCOMBUSTÍVEIS (ANP). Resolução nº 8, de 30 de janeiro de 2015. *Diário Oficial da União*, Brasília, 02 fev. 2015.

AYODELE, T.R.; OGUNJUYIGBE, A.S.O.; ALAO, M.A. Economic and environmental assessment of electricity generation using biogas from organic fraction of municipal solid waste for the city of Ibadan, Nigeria. *Journal of Cleaner Production*, v. 203, p 718-35, 2018. https://doi.org/10.1016/j.jclepro.2018.08.282

ALVES, J.W.S. *Diagnóstico técnico institucional da recuperação e uso energético do biogás gerado pela digestão anaeróbia de resíduos*. 2000. 164 f. Dissertação (Mestrado em Energia) – Programa Interunidades de Pós-Graduação em Energia, Instituto de Eletrotécnica e Energia, Universidade de São Paulo, São Paulo, 2000. https://doi.org/10.11606/D.86.2000.tde-09032012-090952

ALVES, R. *Tratamento e valorização de dejetos da suinocultura através de processos anaeróbios:* operação e avaliação de diversos reatores em escala real. 2007. 172 f. Tese (Doutorado em Engenharia Ambiental) – Universidade Federal de Santa Catarina, Florianópolis, 2007.

AVOM, J.; KETCHA, J.; NOUBACTEP, C.; GERMAIN, P. Adsorption of methylene blue from an aqueous solution on to activated carbons from Palm-Tree Cobs. *Carbon*, v. 35, n. 3, p. 365-9, 1997. https://doi.org/10.1016/S0008-6223(96)00158-3

BHATNAGAR, A; JAIN, A.K. A comparative adsorption study with different industrial wastes as adsorbents for the removal of cationic dyes from water. *Journal of Colloid Interface Science*, v. 281, n. 1, p. 49- 55, 2005. https://doi.org/10.1016/j.jcis.2004.08.076

BOYD, R. *Internalising environmental benefits of anaerobic digestion of pig slurry in Norfolk.* Student research paper. Norwich, Norfolk, UK: University of East Anglia, 2000.

CALCULLI, C.; D'UGGENTO, A.M.; LABARILE, A.; RIBECCO, N. Evaluating people's awareness about climate changes and environmental issues: A case study. *Journal of Cleaner Production*, v. 324, n. 5, p. 129244, 2021. https://doi.org/10.1016/j.jclepro.2021.129244

CAO, X.; GUO, D.; SUN, W.; ZHANG, P.; DING, G.; BIAN, J. Supersonic separation technology for carbon dioxide and hydrogen sulfide removal from natural gas. *Journal of Cleaner Production*, v. 288, p. 125689, 2021. https://doi.org/10.1016/j.jclepro.2020.125689

CASTILHOS JUNIOR, A.B; ZANTA, V.M.; LANGE, L.C.; GOMES, L.P.; PESSIN, N. *Resíduos sólidos urbanos:* aterro sustentável para municípios de pequeno porte. Rio de Janeiro: ABES, 2003.

CHERNICHARO, C.A.L. *Princípios do Tratamento Biológico de Águas Residuárias.* v. 5: Reatores Anaeróbios. Departamento de Engenharia Sanitária e Ambiental. Belo Horizonte: UFMG, 1997.

CRISTIANO, D.M.; MOHEDANO, R.A.; NADALETI, W.C.; CASTILHOS JR, A.B.; LOURENÇO, V.A.; GONÇALVES, D.F.H.; FILHO, P.B. H_2S adsorption on nanostructured iron oxide at room temperature for biogas purification: Application of renewable energy. *Renewable Energy*, v. 154, p. 151-60, 2020. https://doi.org/10.1016/j.renene.2020.02.054

CURIEL-ESPARZA, J.; REYES-MEDINA, M.; MARTIN-UTRILLAS, M.; MARTINEZ-GARCIA, M.; CANTO-PERELLO, J. Collaborative elicitation to select a sustainable biogás desulfurization technique for landfills. *Journal of Cleaner Production*, v. 212, p. 1334-1344, 2019. https://doi.org/10.1016/j.jclepro.2018.12.095

DABROWSKI, A.; PODKOŚCIELNY, P; HUBICKI, Z; BARCZAK, M. Adsorption of phenolic compounds by activated carbon – a critical review. *Chemosphere*, v. 25, p. 1049-70, 2005. https://doi.org/10.1016/j.chemosphere.2004.09.067

DEUBLEIN, D.; STEINHAUSER, A. *Biogas from waste and renewable resources.* 2. ed. Weinheim: Wiley-VCH Verlag GmbH e Co KGaA, 2011.

DOS SANTOS, H.A.P.; DE CASTILHOS JÚNIOR, A.B.; NADALETI, W.C.; LOURENÇO, V.A. Ammonia recovery from air stripping process applied to landfill leachate treatment. *Environmental Science and Pollution Research*, v. 27, n. 36, p. 45108-20, 2020. https://doi.org/10.1007/s11356-020-10397-9

DIAS, G.F. *Pegada ecológica e sustentabilidade humana.* São Paulo: Gaia, 2002.

DÍAZ, E.; ORDÓÑEZ, S.; VEGA, A.; PRADOS, J.C. Comparison of adsorption properties of a chemically activated and a steam-activated carbon, using inverse gas chromatography. *Microporous and Mesoporous Materials*, v. 82, n. 1-2, p. 173-81, 2005. https://doi.org/10.1016/j.micromeso.2005.03.010

DÍAZ, I.; LOPES, A.C.; PÉREZ, S.I.; FDZ-POLANCO, M. Performance evaluation of oxygen, air and nitrate for the microaerobic removal of hydrogen sulphide in biogas from sludge digestion. *Bioresource Technology*, v. 101, n. 20, p. 7724-30, 2010. https://doi.org/10.1016/j.biortech.2010.04.062

ENVIRONMENTAL PROTECTION AGENCY (EPA). *Methane and nitrous oxide emissions from natural sources.* Washington, DC: EPA, 2010.

FAKHRAIE, S.; RAJABI, H. R.; RASHIDI, A.; OROOJI, Y.; GHASEMY, E.; SHAYESTEH ZERAATI, A.; MIRHASHEMI, A. In situ simultaneous chemical activation and exfoliation of carbon quantum dots for atmospheric adsorption of H_2S and CO_2 at room temperature. *Applied Surface Science*, v. 559, n. 6, p. 149892, 2021. https://doi.org/10.1016/j.apsusc.2021.149892

FARGHALI, M.; ANDRIAMANOHIARISOAMANANA, F.J. AHMED, M.M.; KOTB, S.; YAMASHIRO, T.; IWASAKI, M.; UMETSU, K. Impacts of iron oxide and titanium dioxide nanoparticles on biogas production: Hydrogen sulfide mitigation, process stability, and prospective challenges. *Journal of Environmental Management*, v. 240, p. 160-7, 2019. https://doi.org/10.1016/j.jenvman.2019.03.089

GARCILASSO, V.P.; VELÁZQUEZ, S.M.; COELHO, S.T. Geração de energia elétrica a partir do biogás proveniente de aterro sanitário: estudo de caso. *In:* CONGRESSO BRASILEIRO DE ENERGIA, 13., 2010, Rio de Janeiro. *Anais [...].* Rio de Janeiro, 2010. p. 1249-1261.

LANGE, L.C.; AMARAL, M.C.S. Geração e características do lixiviado. *In:* GOMES, L.P. (coord.). *Estudos de caracterização e tratabilidade de lixiviados de aterros sanitários para as condições brasileiras.* v. 1. Rio de Janeiro: ABES, 2009. p. 97-139.

HERNÁNDEZ, S.P.; SCARPA, F.; FINO, D.; CONTI, R. Biogas purification for MCFC application. *International Journal of Hydrogen Energy*, v. 36, n. 13, p. 8112-8, 2011. https://doi.org/10.1016/j.ijhydene.2011.01.055

HU, L.; DU, Y.; LONG, Y. Relationship between H_2S emissions and the migration of sulfur-containing compounds in landfill sites. *Ecological Engineering*, v. 106, p 17-23, 2017. https://doi.org/10.1016/j.ecoleng.2017.05.026

HOWARD, J.R. *Fluidized bed technology:* principles and applications. Bristol: Ed. Adam Hilger, 1989.

KANG, J.W.; JEONG, C.M.; KIM, N.J.; KIM, M.I.; CHANG, H.N. On-site removal of H_2S from biogas produced by food waste using an aerobic sludge biofilter for steam reforming processing. *Biotechnology and Bioprocess Engineering*, v. 15, n. 3, p. 505-11, 2010. https://doi.org/10.1007/s12257-009-0134-8

KAZA, S; YAO, L; BHADA-TATA, P; AND VAN WOERDEN, F. *What a waste 2.0:* a global snapshot of solid waste management to 2050. Urban Development Series. Washington, DC: World Bank, 2018.

KHAN, M.U.; LEE, J.T.E.; BASHIR, M.A.; DISSANAYAKE, P.D.; OK, Y.S.; TONG, Y.W.; SHARIATI, M.A.; WU, S.; AHRING, B.K. Current status of biogas upgrading for direct biomethane use: a review. *Renewable and Sustainable Energy Reviews*, v. 149, n. C, p. 111343, 2021. https://doi.org/10.1016/j.rser.2021.111343

LASTELLA, G.; TESTA, C.; CORNACCHIA, G.; NOTORNICOLA, M.; VOLTASIO, F.; SHARMA, V.K. Anaerobic digestion of semi- solid organic waste: biogas production and its purification. *Energy Conservation and Management*, v. 43, n. 1, p. 63-75, 2002. https://doi.org/10.1016/S0196-8904(01)00011-5

LIMA, R.M.; SANTOS, A.H.M.; PEREIRA, C.R.S.; FLAUZINO, B.K.; PEREIRA, A.C.O.S.; NOGUEIRA, F.J.H.; VALVERDE, J.A.R. Spatially distributed potential of landfill biogas production and electric power generation in Brazil. *Waste Management*, v. 74, p. 323-334, 2018. https://doi.org/10.1016/j.wasman.2017.12.011

LOZANO-CASTELLÓ, D.; CAZORLA-AMORÓS, D.; LINARES-SOLANO, A.; QUINN, D.F. Influence of pore size distribution on metane storage at relatively low pressure: preparation of activated carbon with optimum pore size. *Carbon*, v. 40, n. 7, p. 989-1002, 2002. https://doi.org/10.1016/S0008-6223(01)00235-4

MERCADO, A.G. *Remoção de sulfeto de hidrogênio de biogás em instalação de piloto com óxido de ferro*. 2010. 150 f. Dissertação (Mestrado) – Universidade Federal de Santa Catarina, Florianópolis, 2010.

METCALF & EDDY, INC.; TCHOBANOGLOUS, G.; BURTON, F.L. *Wastewater engineering:* treatment, disposal and reuse. 3. ed. New York: McGraw-Hill, 1991.

MUCHE, H.; ZIMMERMANN, H. *Purification of biogas, deutsches zentrum für entwicklungs technologien*. Eschborn: GATE, Deutsche Gesellschaft für Technische Zusammenarbeit (GTZ) GmbH, 1985.

MIRZABAEV, A.; WU, J.; EVANS, J.; GARCÍA-OLIVA, F.; HUSSEIN, I.A.G.; IQBAL, M.H.; KIMUTAI, J.; KNOWLES, T.; MEZA, F.; NEDJRAOUI, D.; TENA, F.; TÜRKEŞ, M.; VÁZQUEZ, R.J.; WELTZ, M. DESERTIFICATION. IN: SHUKLA, P.R.; SKEA, J.; CALVO BUENDIA, E.; MASSON-DELMOTTE, V.; PÖRTNER, H.-O.; ROBERTS, D.C.; ZHAI, P.; SLADE, R.; CONNORS, S.; VAN DIEMEN, R.; FERRAT, M.; HAUGHEY, E.; LUZ, S.; NEOGI, S.; PATHAK, M.; PETZOLD, J.; PORTUGAL PEREIRA, J.; VYAS, P.; HUNTLEY, E.; KISSICK, K.; BELKACEMI, M.; MALLEY, J. (Eds.). Climate Change and Land: an IPCC special report on climate change, desertification, land degradation, sustainable land management, food security, and greenhouse gas fluxes in terrestrial ecosystems. 2019. https://doi.org/10.1017/9781009157988.005

MURANAKA, C. T. *Combinação de adsorção por carvão ativado com processo oxidativo avançado (POA) para tratamento de efluentes contendo fenol*. 2010. 166 f. Tese (Doutorado em Engenharia Química) – Universidade de São Paulo, São Paulo, 2010.

OLIVEIRA, M.H.A. *Cinética e equilíbrio de adsorção para armazenamento de gás natural*. 2004. 106 f. Dissertação (Mestrado em Engenharia Química) – Universidade Federal de Pernambuco, Pernambuco, 2004.

OLIVEIRA, M.V.C.; CARVALHO A.R. *Princípios básicos do saneamento do meio*. 6. ed. São Paulo: Editora Senac São Paulo, 2005.

PECORA, V. *Implantação de uma unidade demostrativa de geração de energia elétrica a partir do biogás de tratamento do esgoto residencial da USP:* estudo de caso. 2006. Dissertação (Mestrado) – Universidade de São Paulo, São Paulo, 2006.

PELCZAR JUNIOR, M.J.; CHAN, E.C.S.; KRIEG, N.R. *Microbiologia:* conceitos e aplicações. 2. ed. v. 1. São Paulo: Pearson Education do Brasil, 1997.

PELEKANI, C.; SNOEYINK, V.L. Competitive adsorption between atrazine and methylene blue on activated carbon: the importance of pore size distribution. *Carbon*, v. 38, n. 10, p. 1423-36, 2000. https://doi.org/10.1016/S0008-6223(99)00261-4

PELLERIN, R.A.; WALKER, L.P.; HEISLER, M.G.; FARMER, G.S. Operation and performance of biogas-fueled cogeneration systems. *Energy in Agriculture*, v. 6, n. 4, p. 295-310, 1988. https://doi.org/10.1016/0167-5826(88)90003-4

PERRIN, A.; CELZARD, A. MARÊCHÉ, J.F.; FURDIN, G. Methane storage within dry and wet active carbons: a comparative study. *Energy & Fuels*, v. 17, p. 1283-91, 2003. https://doi.org/10.1021/ef030067i

PELUSO, A.; GARGIULO, N.; APREA, P.; PEPE, F.; CAPUTO, D. Nanoporous materials asH_2S adsorbents for biogas purification: a review. *Separation and Purification Reviews*, v. 48, n. 1, p. 78-89, 2019. https://doi.org/10.1080/15422119.2018.1476978

PIZARRO-LOAIZA, C.A.; ANTÓN, A.; TORRELLAS, M.; TORRES-LOZADA, P.; PALATSI, J.; BONMATÍ, A. Environmental, social and health benefits of alternative renewable energy sources. Case study for household biogas digesters in rural areas. *Journal of Cleaner Production*, v. 297, p. 126722, 2021. https://doi.org/10.1016/j.jclepro.2021.126722

REICHERT, G.A. *Projeto, operação e monitoramento de aterros sanitários*. Belo Horizonte: ReCESA, 2007.

SEKAR, M.; SAKTHI, V.; RENGARAJ, S. Kinetics and equilibrium adsorption study of lead (ii) onto activated carbon prepared from coconut shell. *Colloid and Interface Science*, v. 279, n. 2, p. 307-13, 2004. https://doi.org/10.1016/j.jcis.2004.06.042

SCHNEIDER, E.L. *Adsorção de compostos fenólicos sobre carvão ativado*. 2008. 93 f. Dissertação (Mestrado em Engenharia Química) – Universidade Estadual do Oeste do Paraná, Centro de Engenharias e Ciências Exatas, Toledo, 2008.

SUN, Q.; LI, H.; YAN, J.; LIU, L.; YU, Z.; YU, X. (2015) Selection of appropriate biogás upgrading technology - a review of biogás cleaning, upgrading and utilisation. *Renewable and Sustainable Energy Reviews*, v. 51, p. 521-532.

TCHOBANOGLOUS, G.; BURTON, F.L.; STENSEL, H.D. *Wastewater engineering:* treatment and reuse. 4. ed. New York: McGraw- Hill Companies, 2003.

THANAKUNPAISIT, N.; JANTARACHAT, N.; ONTHONG, U. Removal of hydrogen sulfide from biogas using laterite materials as an adsorbent. International Conference on Alternative Energy in Developing Countries and Emerging Economies, Bangkok, Thailand. 2017. https://doi.org/10.1016/j.egypro.2017.10.215

TRUONG, L.V.A.; ABATZOGLOU, N. A H_2S reactive adsorption process for the purification of biogas prior to its use as a bioenergy vector. *Biomass and Bioenergy*, v. 29, n. 2, p. 142-51, 2005. https://doi.org/10.1016/j.biombioe.2005.03.001

WELLINGER, A.; LINBERG, A. *Biogas upgrading and utilization* – IEA Bioenergy Task 24. Paris: International Energy Association, 2000.

YANG, R.T. *Gas separation by adsorption processes*. Stoneham, MA: Butterworth Publishers, 1987.

ZANTA, M.Z.; MARINHO, M.J.M.R.; LANGE, L.C.; PESSIN, N. Resíduos sólidos, saúde e meio ambiente: impactos associados aos lixiviados de aterro sanitário. In: CASTILHOS JUNIOR, A.B. (coord.). *Gerenciamento de Resíduos Sólidos Urbanos com ênfase na proteção de corpos d'água:* prevenção, geração e tratamento de lixiviados de aterros sanitários. Petrópolis: Sermograf Artes Gráficas e Ed. Ltda., 2006. 494 p.

ZHANG, Z.; GUO, L.; WANG, Y.; ZHAO, Y., SHE, Z.; GAO, M., GUO, Y. Application of iron oxide (Fe3O4) nanoparticles during the two-stage anaerobic digestion with waste sludge: Impact on the biogas production and the substrate metabolism. *Renewable Energy*, v. 146, p. 2724-35, 2020. https://doi.org/10.1016/j.renene.2019.08.078

© 2024 Associação Brasileira de Engenharia Sanitária e Ambiental
This is an open access article distributed under the terms of the Creative Commons license.